PMP
Progress in Medical Physics 33(4), December 2022
https://doi.org/10.14316/pmp.2022.33.4.37
eISSN 2508-4453

Review Article

Image Guided Radiation Therapy

Ui-Jung Hwang[1], Byong Jun Min[2], Meyoung Kim[3], Ki-Hwan Kim[1]

[1]Department of Radiation Oncology, Chungnam National University Hospital, Daejeon, [2]Department of Radiation Oncology, Chungbuk National University Hospital, Chungjoo, [3]Department of Radiation Oncology, Chuncheon Sacred Heart Hospital, Chuncheon, Korea

Received September 30 2022
Revised December 12 2022
Accepted December 14 2022

Corresponding author
Ki-Hwan Kim
(khkim@cnuh.co.kr)
Tel: 82-42-280-8362
Fax: 82-42-280-7899

Over the past decades, radiation therapy combined with imaging modalities that ensure optimal image guidance has revolutionized cancer treatment. The two major purposes of using imaging modalities in radiotherapy are to clearly delineate the target prior to treatment and set up the patient during radiation delivery. Image guidance secures target position prior to and during the treatment. High quality images provide an accurate definition of the treatment target and the possibility to reduce the treatment margin of the target volume, further lowering radiation toxicity and improving the quality of life of cancer patients. In this review, the various types of image guidance modalities used in radiation therapy are distinguished into ionized (kilovoltage and megavoltage image) and nonionized imaging (magnetic resonance image, ultrasound, surface imaging, and radiofrequency). The functional aspects, advantages, and limitation of imaging using these modalities are described as a subsection of each category. This review only focuses on the technological viewpoint of these modalities and any clinical aspects are omitted. Image guidance is essential, and its importance is rapidly increasing in modern radiotherapy. The most important aspect of using image guidance in clinical settings is to monitor the performance of image quality, which must be checked during the periodic quality assurance process.

Keywords: Radiation therapy, Image guided radiation therapy, Ionizing image, Nonionizing image

Introduction

Over the past decades, radiation therapy combined with imaging modalities that ensure optimal image guidance has revolutionized cancer treatment. Electron or high energy photon beam therapy, and more recently particle beam therapies, such as proton and carbon ion radiotherapy, have been rapidly commercialized on a worldwide scale. Pertaining to radiotherapy technology, two-dimensional (2D) radiotherapy has already gone to history and 3D conformal radiotherapy are almost obsolete, while both intensity modulated radiotherapy (IMRT) and volumetric modulated arc therapy (VMAT) have now become the mainstream methods used to treat cancer and noncancerous tumors. These technological advancements are backed by the confidence to provide accurate target positioning, which is achieved by the development of efficient image guidance systems. Accurate information of the target position can reduce target volume margin, radiation toxicity to healthy tissues and organs adjacent to the treatment target, and increase the probability of improving the patients' quality of life after radiation treatment [1-3].

Image guidance in radiotherapy is not something new, as every individual effort to secure the target position, and thus improve radiation treatment delivery, prior to the beginning and throughout treatment can be incorporated in this process. The main purpose of image guidance in radiotherapy is to reduce target uncertainty due to errors related

to setting up the clinical procedure and organ motion [4]. The latter consists of intra-fractional organ motion induced by respiration, peristalsis, or bowel gas effects and interfractional motion caused by therapy-induced tumor volume changes, bladder and rectum filling, and intra-abdominal pressure [5-9].

To achieve these goals, various modalities have been used and continue to evolve, such as kilovoltage (kV) image, megavoltage (MV) image, computed tomography (CT), magnetic resonance image (MRI), positron emission tomography, and ultrasound (US). Each imaging modality has its own advantages and limitations [10,11]. In the midst of the rapid evolutionary period of radiotherapy, it is essential to review the effectiveness of these modalities with respect to image guidance, thus establishing a baseline for further developments.

Herein, we first categorized imageguidance modalities according to their characteristics and then briefly introduced each modality. This review solely focuses on the technological viewpoint of these imaging modalities and does not consider any clinical aspects. Therefore, the reader can search more detailed aspect of each modality and clinical advantages or drawbacks or outcomes if you like to look into more.

Classification of Image Guidance Technologies in Radiation Therapy

Image guidance technologies are significantly diverse, rendering their classification challenging. Image guided radiation therapy (IGRT) can be distinguished into the following four systems, each one having different characteristics and imaging goals: cone beam CT (CBCT), fan beam CT (FBCT), planar imaging, and nonionizing visualization [12].

Verellen et al. [13] described the evolution of IGRTs by listing IGRT techniques in chronological order of development. In 1969, Haus et al. placed a radiographic film to the distal end of a patient during treatment to assess of intrafractional uncertainty on the assumption that set up error correlated with clinical follow-up [14, 15]. To improve the accuracy of imaging systems in identifying targets and organs at risk (OAR) adjacent to the target, hypofractionated radiation therapy gradually replaced the conventional fractionation scheme, from which various treatment approaches have emerged such as stereotactic body radiotherapy (SBRT), an extreme form of hypofractionation, and intensity modulated radiotherapy (IMRT), whose radiation doses are higher and more effective [16]. In addition, imaging modalities can be classified according to their interfraction motion or intrafraction identification [17,18]. Another classification may involve MV, kV, and non-radiographic approaches, or planar and volumetric imaging [13].

Goyal and Kataria [19] reported the two major roles that imaging systems should have for radiotherapy: to define the target accurately and get periodic intra- and intermovement information regarding the target position. The authors also highlighted the role of nonradiation based systems, such as US, camera-based, optical tracking systems or electromagnetic tracking systems, MRI-guided and ionization-based systems, such as electronic portal imaging device (EPID), CBCT, fan beam MVCT, hybrid systems for real time 4D tracking as CyberKnife system or real time tracking radiotherapy (RTRT, Mitsubishi Co Ltd, Tokyo, Japan) systems. Furthermore, infrared optical positioning systems and combinations with kV radiographic systems could be placed in another category.

Keall et al. [20] showed that real time 3D image guidance techniques, such as kV intrafraction monitoring, coupled MV and kV imaging (MV/kV), coupled optical and sparse monoscopic imaging with kV X-rays, workflow and quality assurance (QA) for each technique.

Despite the various methods of categorizing imageguidance technologies, this review initially distinguishes IGRT into ionizing and nonionizing methods, and then further divides ionizing methods into kV and MV imaging, and nonionizing methods into MR, US, optical vision, and radio frequency (RF). Fig. 1 illustrates the classification method employed in this paper.

1. Use of ionizing radiation

We then categorized imaging modalities that use ionizing radiation based on their respective energies, such as kV/MV imaging.

In KV imaging, the device is attached to the machine, wall or ceiling, whereas MV imaging includes both planar imag-

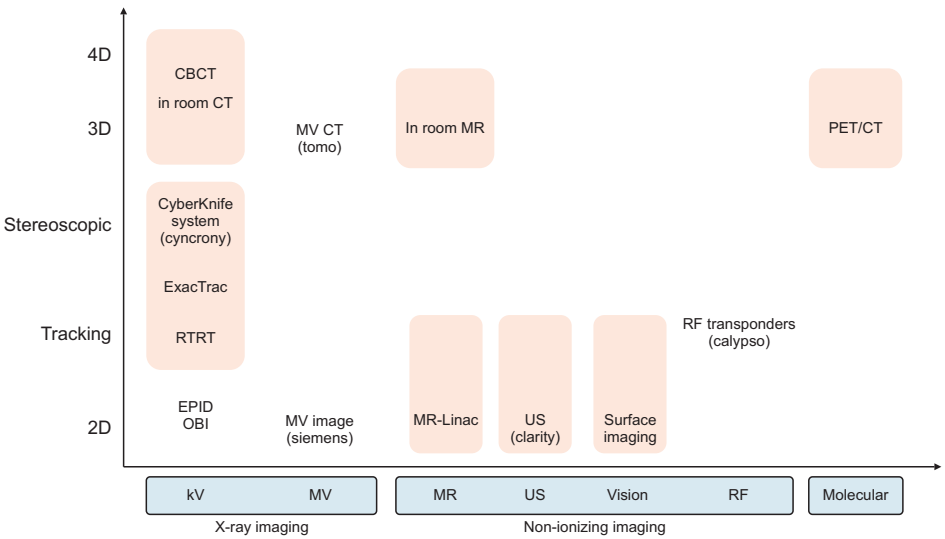

Fig. 1. IGRT techniques categorized based on their characteristics. MR-Linac, US, and surface imaging are categorized as 2D and tracking imaging methods because their tracking ability is limited in 2D coordinates to date. 2D, two-dimensional; CBCT, cone beam computed tomography; CT, computed tomography; EPID, electronic portal imaging device; IGRT, image guided radiation therapy; MR-Linac, magnetic resonance linear accelerator; OBI, onboard imager; PET/CT, positron emission tomography/computed tomography; RF, radio frequency; US, ultrasound.

ing and MVCBCT.

1) kV imaging

The first recorded application of a kV imaging device for radiotherapy purposes goes back to the era of teletherapy with the use of cobalt isotopes. This review only focuses on imaging devices used for clinical linear accelerators (Linacs). Since 1958, when Weissbluth et al. [21] reported the integration of a retractable kV X-ray tube into the head of a Linac, kV CBCT is the most commonly used imaging system for IGRT verification.

(1) kV planar imaging

The kV imaging system consists of a kV radiation X-ray tube, which is mounted orthogonally to the direction of the treatment beam, and a detector panel [20,22]. The greatest advantage of this approach is that images of the day have a significantly higher quality than MV portal images that use an MV detector panel. Consequently, images produced from kV devices are similar in quality to those used for diagnostic purposes.

However, the geometry of this low voltage imaging system hinders the exact visualization or verification of the treatment beam because the combination of a kV X-ray tube with a detector panel does not include beam-limiting devices, such as multi leaf collimators (MLCs), which allow for precise field shaping. Therefore, images taken by the low-voltage X-ray tube are limited because the shaping the exact field size to the treatment. kV images evaluate the position of the patient based on the treatment isocenter [22-24]. but an uncertainty exists regarding the precision of the isocenter position and field placement. Consequently, the relationship between kV imaging and treatment isocenter should be assessed using an alternative method such as treatment planning software.

As previously mentioned treatment beam verification is one of the fundamental limitations of kV imaging, which can subsequently enable the inclusion of the kV imaging dose to the radiation dose delivered to the patient. Fortunately, the kV imaging dose is normally much lower than the MV imaging dose. Therefore, the kV imaging system is very commonly used in IGRT due to the superior image quality of low-voltage X-ray images [22].

Gantry-mounted is the most common arrangement in kV imaging systems where both the X-ray tube and the detector panel are placed together on the gantry. An alternative arrangement is to place the system out of the gantry, the X-ray tubes on the floor, and the detector panels on the ceiling in front of the gantry [25,26]. This system obtains stereoscopic images that enable accurate analysis of patient misalignments even though coordination necessitates rotational conversion. One of the advantages of this system is that images can be obtained independently of the gantry angle, even allowing continuous imaging during treatment by rotating the gantry in case of the arc technique. An additional advantage is that the rotation of the treatment table

does not affect the obtained images. Therefore, a precise setup image of the patient can be acquired with this system when the gantry is angled and the table is rotated.

(2) CBCT

Compared to the conventional CT, which uses a fan-shaped beam, CBCT is a radiographic imaging modality that uses cone shaped X-ray beams with a single 360° scan in order to reconstruct 3D volumetric images. The image quality is similar but not better of that of CT because CBCT systems are intrinsically more prone to scattering and the generation of artifacts. There are specific differences in the acquisition methodology between CBCT and CT, including the rotation technology, scanning speed, and table movement. For instance, contrary to the standard in-room helical CT equipment, CBCT allows the acquisition of imaging data in one revolution at a fixed table position. This in turn limits the maximum scan length to the maximum field side generated by the X-ray tube, which can be a significant issue when treating volumes larger than the maximum field size of the tube [27,28].

Although CBCTs generally use kV energies, MV energies can also be used for the acquisition of volumetric images. With CBCT, bone anatomies, soft tissues, or fiducial markers can be visualized to match the reference image [29-31]. CBCT using MV energies will be discussed in a later section.

(3) In-room CT or CT on rails

CT on rails or in-room CT is a system where the diagnostic CT scanner is placed in the same therapy room with the radiation treatment machine (Linac) [32,33]. In general, the CT scanner moves on rails along the scan axis on the opposite side of the Linac without moving the patient. After the scanning process is completed, CT on rails returns back to its original position and the treatment table is positioned back as well to prevent collisions throughout treatment.

The major advantage of this system is that it facilitates the localization of patient position during radiation delivery, thus enabling the acquisition of high-quality diagnostic images without any limitations to the scan length. However, this system also has some inherent limitations. The cost of purchasing and maintaining a diagnostic CT is higher than that of other imaging modalities, such as diagnostic modalities where the CT scanner is attached to the Linac head or use planar imaging, and the higher cost of preparing the treatment vault due to the requirement for a wider space. In addition, possible patient movements during the translation process between the Linac and the CT on rails may also cause greater setup uncertainty despite the fact that their respective distance is minimized.

2) MV imaging

(1) Concept of MV imaging

MV images are generated by high photon energies such as 2.5, 4, and 6 MV, using the same source of radiation as the treatment one. Compared to kV imaging, the principal advantage of this system is that it minimizes geometrical errors. The kV tube is orthogonal to the MV tube. In addition, metal artifacts can be reduced, allowing clinicians to obtain images with minimal distortion from patients with prosthetics such as dentures [34]. However, the contrast is significantly lower than that provided by kV imaging.

In recent years, low MV energy beams have been used for the generation of high quality images in clinical trials.

EPID are necessary for detecting the MV beam produced by the Linac. EPID are the preferred tools for image verification, in terms of aligning digitally reconstructed radiograph images created by CT simulations before treatment with MV images, and verifying patient positioning for radiotherapy [19,35].

(2) MV portal imaging

As previously mentioned, EPID is used to obtain images from low energy MV beams. However, when high energy MV beams are used, a significant portion of radiation is delivered to patients through Compton scattering, leading to the generation of low-quality images [36]. Instead, 2D projection imaging allows the precise identification of the patient's position with respect to the radiation beam. Previously, kV portal imagers have been solved by using together. However, kV portal imagers generate images from auxiliary devices that are not placed on the Linac, thus increasing the risk of potential inaccuracies in patient position.

Metal artifacts are caused by patients wearing metal prostheses [37]. To solve this issue, low energy portal imagers,

such as 2.5 MV, are widely used in clinical trials because X-rays at that energy range can interact with a higher probability of photoelectric effect than that of high energy portal imagers (6 MV or more). This will in turn produce images with better quality, higher contrast and sharpness, especially in bony anatomical structures.

(3) MVCBCT

MVCBCT is used to reduce setup errors and improve the overall treatment ratio. This is accomplished by comparing the MV imaging beam with planning CT images to assess whether patients are in the optimal treatment position. The CT method uses a slice-by-slice registration that provides precise patient setup [38].

The first commercially available MVCBCT systems were the Siemens Oncor and Artiste platforms. MV imaging can also be used with helical tomotherapy, which integrates a Linac and a MVCT.

MVCBCT where images are acquired with a normal energy of 4 MV. The Halcyon system was recently released by Varian Oncology Systems (Varian, Paloalto, CA, USA) with the following features: 15 seconds rotation time, 800 MU/min nominal dose rate, dynamic MLC with 5 cm/s leaf speed, and 6 MV treatment energy flattening filter free (FFF) [39]. Although this system uses a single energy of 6 MV, it also offers the option for adding an on-board kV CBCT imager, which, however, increases the cost of radiotherapy [40].

The advantage of MVCT is that it uses the same beam line as the treatment one, which makes it possible to minimize potential geometrical errors with a treatment plan and facilitate a comparison with the 3D planned CT images. In addition, the imaging dose of MVCBCT can be considered in the actual treatment planning process because the imaging beam has already been modeled as a treatment beam by the treatment planning system. Imaging volumes ranging from 2–15 cGy per scan have been reported in literature. In case of sufficient image quality with 2.5 MVCBCT images for bony alignment, the MU value for the head, thorax, and pelvic regions was found to be 2–3 MU compared to the 26 MU reported with a 6 MVCBCT scan [41].

In terms of image quality, MVCBCT and MVCT images have less contrast than those of kV CT. However, both images are affected less by metal artifacts. Also, it has been shown that images obtained with MV energies can delineate anatomical structures and verify patient positioning [30,40].

(4) MV tracking

In radiation therapy, the movement of internal organs and patient respiration are responsible for potential differences between planned and irradiated volumes, differences that may cause treatment failure. To solve this problem, it is necessary to observe the anatomical structures constantly and match the radiation field with the planning target volume. Using a statistical approach, tumor motion in 3D could be estimated through limited MV projections [42]. For example, it has been shown that this motion can vary in magnitude in patients with prostate cancer. MV imaging and a motion tracking are required for monitoring tumor motion in real time [43]. MV tracking is also known as cine EPID, and refers to a treatment modality in which radiation is only delivered when the tumor site is in the treatment radiation area. However, it is still difficult to irradiate accurately the tumor in real time by tracking its movement. In recent years, artificial intelligence has been introduced in clinical settings to predict tumor movement or patient breathing patterns, and novel technologies that could ensure precise target irradiation are being studied [44].

2. Use of nonionizing radiation

1) MRI

Image guidance with kV imaging systems, which are the most commonly used systems in recent days, cannot visualize soft tissues, especially in the abdomen and pelvic area, because X-ray images do not contain functional information. Although 4D CBCT can be used for the assessment of intrafraction motion during treatment, the long image acquisition time and the ionizing nature of the X-rays can cause significant issues to the resulting imaging. On the contrary, MRI has better soft tissue visualization, which enables this medical imaging technique to easily distinguish targets from critical structures near the target. An additional advantage of MRI is that it does not use ionizing radiation, and thus it is considered a noninvasive process. The superior soft tissue contrast allows for continuous real time

imaging, which can be used for gating or tracking radiation therapy without surrogate tracking markers on the patient's body. Quantitative imaging is an additional aspect of MRI, which can be a useful tool for tumor response assessment during treatment, indicating the success of real time adaptive therapy. However, MRI has its own drawback as well, such as the requirement of long scanning times for image processing, distortion correction and scale calibration, the necessity to implement MRI and RF shields to the machine and the whole treatment vault, and extra caution regarding MR safe immobilization to allow a reproducible setup for patients [18,45].

In radiotherapy, MRI can be used in target delineation and planning before and during the treatment process, dose calculation, patient setup during treatment delivery, position monitoring, internal organ monitoring, and tumor movement monitoring during the treatment delivery, and treatment response assessment after treatment [18,46-48].

Special precautions are necessary when using MRI, especially because radiation oncology staffs are generally not familiar with the safety precautions required for working with the magnetic field. Staff must have appropriate training to enter MRI zones and consider both MR and radiation safety concerns.

The absence of a symmetric radiation beam profile in the MR environment induces slight changes in the depth dose, shallower maximum dose depth, wider penumbra, and increased dose to the interface between tissue and air (electron return effect) [49-51].

Integration of 6 MV Linac with an 1.5 T MRI system was attempted by Raaijmakers et al. as early as 2004 [49,50,52]. Nowadays, there are several commercialized Linac models combined with MRI systems as an image guidance tool. The first attempt to use MRI in radiotherapy settings was MR on rails, where the MRI scanner is allowed to travel inside the vault in the vicinity of the Linac [53].

(1) MR on rails

The first attempt to use MRI as an imageguidance tool in radiotherapy was to install an MRI very next to the radiotherapy treatment room and allow it to move into the radiotherapy vault when necessary. The Princess Margaret Cancer Centre are the most comprehensive facilities in the world where a 1.5-T MR scanner is mounted on a rail, operating as an MR simulation, MR-guided brachytherapy with a MicroSelectron (Elekta, Stockholm, Sweden) iridium-192 source (10 Ci) enclosed, and MR-guided external radiotherapy with TruBeam (Varian) [54]. Similar to the design of CT on rails for external radiotherapy, MR on rails can translate a 3.1 m long between the isocenters of the Linac and MRI. Because an independent conventional MRI system with Linac is typically used, the MR on rail system lacks the functionality features that the comprehensive MR-Linac system has, such as an online adaptive planning, imaging, and tumor tracking system during treatment. However, systems such as MRIdian (ViewRay, Denver, CO, USA) or Unity (Elekta, Stockholm, Sweden) have managed to include this feature in the integrated form of MRI and Linac.

(2) MRIdian

The first commercial integrated MRI-guided radiation therapy system was introduced for patient treatment processes at the Washington University (St Louis, MO, USA), in 2014. In the initial system model, the radiotherapy delivery system consisted of three Co-60 sources with three 10.5×10.5 cm^2 fields at the isocenter controlled by a double stack and double focus MLC system and the initial dose rate was approximately 550 cGy/min [55].

The ViewRay system consists of three main components, namely the MRI system, radiotherapy delivery system, and adaptive radiotherapy treatment planning system. The first system has three cobalt isotopes as the radiation therapy system and a 0.35-T MRI system with a double-doughnut design with a 50-cm field of view (FOV). Co-60 sources are set apart 120° from one another that can freely rotate ±60° from their initial position [55].

This MRI system has a 70-cm bore diameter, which provides a 50-cm imaging FOV, and it is operated by the True Fast Imaging with Steady State Precession (TRUFI) sequence during clinical imaging. This system also can also perform real time imaging for one or three planer images of a sagittal cross section with a frame rate of four frames per second.

The Co-60 source does not affect the magnetic field, and the radiation generated from these isotopes is not influenced by the magnetic field as well. Therefore, the only fac-

tor that needs to be considered is the effect of the magnetic field to the radiation dose inside the patient body.

In other way, radio isotopes have limited in reducing their size which is one of the main causes of an increased penumbra, and needs regular replacement due to decreasing dose rate induced by radiation decay, which of course increases the maintenance cost. The beam penumbra was measured to be approximately 2–4 times broader than the one in the conventional Linac [56]. The use of three isotopes, which are deployed symmetrically around the isocenter, mitigates the relatively low dose rate operation; however, MLCs for each source allow a complication of mechanical operation. Consequently, the ViewRay system has now shifted to a single Linac-based system.

The Linac-based system can maintain a continuous high dose rate, and the single MLC used can reduce errors during the operation. A few technical specifications include an FFF X-ray beam of 6 MV, a 90-cm SAD, a 600-cGy/min dose rate at the isocenter, double focus and double stacked MLC composed of 138 leaves with a maximum field size of 27.4×24.1 cm, whose penumbra is as small as 1.75 mm at a 2×4.15 mm field size.

The 0.35-T MRI operates with a fast slew rate of 200 T/m/s. A 217-cm long bore length covers the entire length of the patient, while a flexible RF coil can transmit RF energy to any site. Its capability to take real time sagittal images with 4 fps during irradiation always enables the gating treatment based on MRI guidance. MR images obtained for patient positioning/setup calculate the expected dose distribution to be delivered to patients, reoptimize segments for predetermined fields, and reoptimize both the gantry angle and MLC if necessary [57].

(3) Unity

Another MR-guided Linac system manufactured by Elekta hybrided with a 1.5-T Philips MRI is now installed globally after its recent commercialization. The Unity system uses a 7-MV energy X-ray positioned outside the magnetic bore with a dose rate of 500 cGy/min; hence, the radiation beams are delivered to the patient after passing through the magnet [54,58,59]. This system has a relatively long SAD of 143.5 cm and 160 leaves MLC moving in a direction parallel to the axis of the magnet. The MRI system provides various sequences, such as T1-weighted, T2-weighted, and diffusion weighted, with the superior functionality of performing real time imaging in three planes (axial, sagittal, and coronal) simultaneously. Gating delivery guided by real time MRI is not yet installed, but its expected to be adopted soon. In terms of adaptive radiation therapy, the Unity system provides two types of adaptive therapy modes: adapt to position (ATP) and adapt to shape (ATS) workflows. Regarding the ATP workflow, daily delineation is neither needed nor possible because the only parameter updated compared to the pretreatment CT is the isocenter position. In contrast, in the ATS workflow, volumes around the target can be recontoured based on the daily MRI for treatment plan adaptation.

The ATP workflow allows for plan adaptation solely based on the online patient's position on the table. Consequently, the simulated CT image is matched with the online MRI via rigid image registration, and when this process is completed, the isocenter position is updated based on the daily MRI image. Then the dose distribution is recalculated or reoptimized to reproduce or improve target coverage in the original plan. All these processes use simulation CT and predelineated contours, and thus recontouring is unnecessary because plan adaptation is based on the original predelineated contours [60].

The ATS workflow allows for plan adaptation according to the patient's new anatomy, and the treatment plan is optimized based on the daily MRI image and contour adjustment. The first step is the same as in ATP, i.e., image registration between the pretreatment CT and MRI image of the day. The predefined contours are then automatically propagated by deformable image registration onto the new MRI image, and if necessary, the propagated contours are edited or confirmed by a radiation oncologist. Electron densities (EDs) are assigned to the structures based on the average ED of the corresponding contours on the simulation CT, the plan is then recalculated or reoptimized based on the MRI image of the day, and the contours are adjusted. The list of the objective functions for optimization remains unchanged in the ATS workflow. Similar to the ATP workflow, the ATS workflow has multiple options for plan recalculation and reoptimization [60].

(4) Additional MRg Linacs

Two other types of MRg Linacs are being developed on the research base: the Australian MRI-Linac and the Aurora-RT (MagnetTx, Edmonton, Canada).

The Australian MRI-Linac program was recently implemented at the University of Sydney, Australia to exploit the ability of MRI in providing functional information from both spatial and temporal patient images and adaptive radiotherapy. This system uses a 1.0-T open bore magnet with a 82-cm diameter and a 50-cm gap. The spectrometer and control system are provided from Siemens, and the 6-MV Linac with Millennium 120 leaf were delivered from Varian. The researchers employed an inline orientation in which the Linac is aligned with B0 and the patient is placed in-between the magnet gaps to minimize the effect of the B field on both the Linac operation and the modified dose inside the body [61].

Another research-based MR-Linac has integrated a Linac onto a biplanar rotating MR system. The researchers have tried both configurations (radiation is perpendicular or parallel to the magnetic field direction of the MRI) and showed that the parallel configuration could reduce the exit skin dose and dosimetric hot spots that are present in the perpendicular configuration of other systems and which are caused by the electron return effect. With the 6-MV Linac, they optimized the magnetic field strength to 0.6 T, which they believe it is the only way to eliminate the radiation hot spots developed at the air-tissue interfaces within the lung or bronchus [62]. This system will soon become commercialized under the name of Aurora-RT at MagnetTx Oncology Solutions Ltd.

The most outstanding difference between these two MR-Linac systems combined with an open magnet configuration is the rotating part of the system. In the Australian MRI-Linac, both the magnet and the Linac are fixed and the patient can be rotated to achieve conformal delivery of the radiation beam. On the contrary, the Aurora-RT has a rotating MR magnet and the patient is not moved during treatment.

A hybrid MRI/Linac system is a technical challenge because the MRI and the Linac affect one another, degrading the quality of MRI images and inducing significant instabilities on the Linac operation.

To reduce the effect of the RF wave generated from the Linac to the homogeneity of the magnetic field, and thus to the resultant MR images, the RF shielding technique is commonly used. The shield consists of carbon fiber and copper material, which absorbs and reflects the RF wave, respectively, preventing it from reaching the imaging space of the MRI system. All Linac components, such as RF generator and modulators, are placed symmetrically around the MRI magnet bore to minimize magnetic field distortion and secure the integrity of the field. Things that any movement of metallic components is not allowed during MR imaging limits to only step and shoot delivery with MLC and prohibits VMAT technique in IMRT delivery.

Furthermore, the impact of the magnetic field to the electronic circuit and RF system of the Linac can be prevented by “hiding” the Linac from the magnetic field. Ferromagnetic materials and mu-metals can reduce the magnetic field around the Linac almost to the geomagnetic level.

MRI is one of the most prominent imaging modalities in IGRT, but certain improvements should be made to propel its widespread use. Accuracy in dosimetric calculations and highly modulative dose distribution could compete with the high quality dose distribution generated from the state of the art Linac system equipped with innovative hardware and artificial intelligence (AI)-aided software [63].

2) US

Current research has also been focusing on the adaptation of US imaging to radiation therapy as an image guidance tool because this modality can provide 2D, 3D, and anatomical imaging, and real time monitoring. Although not widespread, US is now being used in radiation therapy for patients with prostate, bladder, breast, and liver cancer [64,65].

US imaging also provides a good soft tissue contrast and allows for contouring of organs, such as the prostate, which cannot be adequately distinguished in CT. US a real time image modality in which images are continuously reconstructed and visualized during the image acquisition process.

Although US is a nonionizing imaging modality, which does not induce additional harm to patients treated, and it is a relatively cost effective, the reason why US imaging

is not widely used in clinical settings is due to its distinct drawbacks. For instance, US assumes that the average speed of sound remains the same for all different tissues during the imaging process, adding a distance uncertainty to the respective images. Geometric uncertainty is also enhanced when the US travels deeper in the respective tissues. Furthermore, it has low tissue accessibility due to high absorption by dense materials, such as bone, and homogeneous low-density materials such as air. In addition, the frequent occurrence of occurring artifacts on US images and the strong user dependency, which is due to the requirement for manual operation, render the US difficult to adapt to radiotherapy. Finally, to achieve sufficient acoustic coupling between the probe and the patient body, an acoustic coupling medium, such as water or gel, is typically applied to the patient's skin, which is not compatible with radiation therapy.

The prostate is one of the most widely used sites for US imaging, which can be divided in three types: transrectal US imaging (TRUS), transabdominal US imaging (TAUS), and transperineal US imaging (TPUS) [66].

In TRUS, the probe is placed inside the rectum through the anus. Although it is a minimally invasive imaging procedure with good image quality of the prostate, rectal filling is required, and the potential existence of air bubbles in the rectum may result in poor images. Usually, the probe is guided by fiducial markers during the simulation, while monitoring of inter and intrafraction organ motion during the treatment is less commonly used. TRUS also plays a crucial role in brachytherapy in prostate cancer. In addition, although other imaging modalities can be significantly more effective in external radiotherapy than US, high dose rate or low dose rate prostate implants are limiting these imaging modalities in terms guiding applicators and needles.

In TAUS, the probe is placed on the abdomen and measures the prostate volumes obtained from TRUS imaging, by using the acoustic window of the bladder; however, this implies that patients will need to have a full bladder, which may cause a significant discomfort to the patient. This approach is unavoidable to far location of the probe from the prostate, which might affect the image quality in case of heavy adipose tissue in obese patients. It could be said that this approach is suitable for interfraction monitoring, yet it is very challenging as the probe may be in the beam path during treatment.

Finally, in TPUS, the probe is placed on the perineum and a semi-full bladder is required to obtain good quality images. In addition, the probe does not interfere with the treatment beam, and is thus a good configuration for monitoring intrafraction motion during the treatment.

Few US systems have been commercialized for radiotherapy, including the SonArray system (Varian), B-Mode Acquisition and Targeting system (Best nomos, Pittsburgh, PA, USA), and Clarity (Elekta). Clarity Autoscan is the only commercial system used in the clinical field offering motorized control of the sweeping motion of the 2D probe (m4DC7-3/40, center frequency of 5 MHz and a probe tracking system attached to a base plate on the CT or Linac table [67-69]. The 3D volume is evaluated at the simulation stage, prior to the treatment planning process. A full sweep image is obtained and compared with the simulated image for the calculation of isocenter displacement, accounting for the interfractional motion of the prostate. Real time imaging of this volume allows 3D monitoring of the prostate movement during the treatment.

US images have a geometric difference of approximately 5–10 mm from other 2D or 3D volumetric imaging modalities such as CBCT and CT. Latency of approximately 45–220 ms between the motion of the US phantom and the tracking in real time monitoring and prostate displacement (in TAUS) of approximately 1–3 mm due to pressure from the probe have been reported. In contrast, there is no expected displacement of the prostate or other OAR around it in TPUS imaging, due to the fact that the probe does not need to be removed during the dose delivery. Differences in imaging quality among different operators must be considered in US imaging. Furthermore, inter- and intra-operator variability of approximately 1–2 mm can be assumed in terms of matching the US image to other images, which can be improved by further training and experience [66-69].

3) Surface imaging

In recent years, the clinical use of surface guided radiation therapy (SGRT) has rapidly increased. SGRT systems use optical surface scanning of patients for patient positioning prior to the start of the treatment, but also for patient

monitoring during treatment, including respiratory gating. Such systems can substitute the patient setup laser and imaging systems, such as electronic portal, on-board imager, or cone beam CT and conventional respiratory gating signal generating systems individually or as a whole.

Generally, the SGRT technique uses a projector and one or several camera units to scan the surface skin of the patients. A reference surface image around the treatment isocenter position taken at the time of simulation is necessary for calculating the potential shift in the patient position in six dimensions, including both translational and rotational directions. Optical scanning of the patient's surface is aided by laser scanners, a depth camera with time of flight technology, stereovision technologies, and structured light systems [70-72].

Although there are some differences pertaining to the technique employed and the actual process among models, the advantages of surface image guidance are submillimeter accuracy, noninvasivess, nonionization, etc. Surface image guidance is only tracking the patient surface and not tumors or organs inside the patient. Therefore, a discrepancy between surface and tumor movements may exist. Correlation between tumor and surface motion depends on the respective site, and thus the surface cannot be always a reliable surrogate parameter.

There are some intrinsic disadvantages of surface imaging. An optical system is used to scan the patient's surface, which is influenced by the surrounding light intensity of the room, the light field from the gantry head, and the skin tone of each patient. A region of interest (ROI), which in this case is the skin surface of the patient, should always be visible to the camera and should not be covered with a blanket during the treatment. Therefore, patients may feel discomfort, especially when a sensitive area needs to be constantly exposed or due to low temperatures in the treatment room. During treatment monitoring, the monitoring signal can vary according to the location and shape of the ROIs set. The accuracy of this process is reduced the flatter the ROI surface becomes and with no surface modulated.

Many clinical reports have been published using surface image guidance, including the monitoring of breasts shape and position, cardiac sparing with deep inspiration breath hold in left breast radiotherapy, surface guidance patient setup in whole breast and accelerated partial breast irradiation, open mask immobilization using SGRT in head and neck (H&N) cases, breath hold lung SBRT, and Pelvis RT [73-75].

Several image guiding systems have become commercial globally. Among these systems, the AlignRT (VisionRT Ltd, London, UK), Catalyst (C-RAD, Uppsala, Sweden), Identify (Varian), and the ExacTrac Dynamic (BrainLab, Munich, Germany) have already been introduced in Korea so far. The following sections will briefly introduce the AlignRT and Catalyst and ExacTrac Dynamic systems.

(1) AignRT

The AlignRT system, which is available under the VisionRT brand name, is installed in the treatment room with three pods mounted at the ceiling, one central and two lateral pods. Each pod contains two camera sensors and a projector enabling real time 3D surface reconstruction. Frame rates for images updated by cameras can reach up to 25 fps. A 3D body surface of the patient generated based on the planning CT is exported to the AlignRT system as a reference image. ROIs could then be set on the body surface to monitor the patient's position during the treatment. The average difference of the position on the ROI area is calculated with six degrees of freedom using a rigid image registration algorithm. The definition of ROIs can affect the respective results, therefore, it is important to establish a ROI that best represents patient and tumor motions, and ensure good detectability by the cameras. For example, in patients with breast cancer the ROI includes the breast with an isotropic margin of a few centimeters. Sometimes ROIs are modified to ensure proper visualization and optimize the reasonable positioning error calculated. ROI monitoring on the ipsilateral breast has been shown to be more accurate than monitoring both breasts [76].

(2) Catalyst

The Catalyst system consists of three high-power light emitting diode projectors of different colors and different purposes. A projector using near-visible violet light (λ=405 nm) reconstructs the surface on the patient skin, while projectors using green (λ=528 nm) and red (λ=624 nm) light are used for live feedback of the patient's posture. The near-

visible violet light is projected as sequenced lines onto the patient's surface to be scanned. The irregular surface of the objects scanned may distort the sequenced projected lines detected by a charged-coupled device (CCD) camera. Due to the fixed geometry between the projector and the CCD, optical triangulation can be used to reconstruct a 3D surface of the patient's surface. Patient setup is performed in two steps prior to the treatment: first, patient posture correction is accomplished using surface image matching and then isocenter position adjustment is performed using a deformable algorithm matching to the reference image. To correct patient posture, the Catalyst system matches the current patient's surface, which is updated in real time, with the reference surface, which is limited within a predetermined volume, and then calculates a distance map between the surfaces. As the distance of the two surfaces differs from the predefined level, the system creates a 3D color map that represents spatial out of tolerance, which is subsequently projected onto the patient's skin by the projectors. The therapists can then correct the patient's posture and position by assessing the projected transparent color map on the patient surface [77-79].

(3) ExacTrac Dynamic

Recently, a somewhat different type of surface image guidance system has been developed and commercialized, which is combined with a thermal tracking system. More specifically, in the ExacTrac Dynamic, a stereoscopic X-ray system, optical surface tracking system, and thermal tracking system are all combined in a single system. This system uses a conventional x-ray imaging system with two x-ray tubes mounted on the floor and two flat panel detectors mounted on the ceiling of the treatment room, and surface imaging is performed with optical and thermal cameras mounted on the ceiling, which detect visible surface images of the patient and infrared waves radiated from the body, respectively. Thermal images of the patients might reduce the registration sliding effects for surface imaging and improve position accuracy [80].

4) RF

Target localization is accomplished by two methods which are either image or fiducial based. Image based localization utilizes medical images taken by a radiographic method, such as kV and MV imaging, 2D or 3D imaging, and other images such as US. One of the fiducials for target localization could use RF signals from the transponder implanted near the treatment target. These signals can be tracked by a receiver array positioned outside the patient.

The Calypso 4D System (Varian) is an example that uses radiofrequency waves for monitoring the prostate during each treatment fraction. Three small electromagnetic transponders or beacons are implanted into the prostate using an US-guided transrectal approach, and the beacon transponders inside the prostate communicate with the Calypso 4D using radiofrequencies during the radiation treatment [81-83].

However, communication with transponders implanted deeper than 27 cm underneath the skin is not feasible. Furthermore, metallic structures, such as hip prostheses, may interfere with this communication if they happen to be on the transponders path. Nonetheless, this is nonionizing radiation method with the capability of real time tumor tracking, which increases the accuracy of tumor position and reduces treatment margins for dose escalation with minimal tissue toxicity.

Many studies have shown that real time tracking of patients is an essential advantage for the success of radiation treatment, especially when it comes to the prostate, by tracking intrafraction motion during treatment fractions [82-84].

Discussion and Conclusion

Image guidance in radiation therapy incorporates imaging techniques during each treatment session and can reduce target margins and increase the radiation dose delivered to the target, while sparing normal tissue that is adjacent to the target from exposure to a high radiation dose. Various imaging modalities have been used. Some of a modality has prior visibility in soft tissue to the other one which has a distinctive bone discriminability for example. Bone is a good radiographic marker for image guidance in setting up the radiotherapy patient. However, most of the target volume is bound to contain soft tissue, which can easily shift the true location of the target site. Consequently,

if high quality images are obtained before each radiation therapy treatment session, the target can be matched with the planning images, rather than the bone, facilitating a more accurate treatment process. On the contrary, matching the bone can provide higher accuracy of radiation delivery in cases of brain and H&N tumors, or based on the internal target volume in patients with lung cancer.

Therefore, image guidance modality should be carefully selected by considering the treatment site, availability, cost, and applicability.

To maintain the optimal accuracy of image guidance, QA focusing on the imaging modality used is essential because it is frequently overlooked compared with the treatment machine. Image guidance is now becoming a standard protocol, specifically for adaptive radiation therapy.

In this respect, further studies are necessary for the identification of the optimal target margin in each modality and each treatment site.

Acknowledgments

This work was supported by the Chungnam National University Hospital Research Fund, 2019-CF-033.

Conflicts of Interest

The authors have nothing to disclose.

Availability of Data and Materials

The data that support the findings of this study are available on request from the corresponding author.

Author Contributions

Conceptualization: Ui-Jung Hwang, Byong Jun Min, and Meyoung Kim. Data curation: Ui-Jung Hwang, Byong Jun Min, and Meyoung Kim. Formal analysis: Ui-Jung Hwang and Ki-Hwan Kim. Funding acquisition: Ki-Hwan Kim. Investigation: Ui-Jung Hwang, Byong Jun Min, and Meyoung Kim. Methodology: Ui-Jung Hwang, Byong Jun Min and Meyoung Kim. Project administration: Ui-Jung Hwang and Ki-Hwan Kim. Resources: Ui-Jung Hwang, Byong Jun Min, and Meyoung Kim. Software: Ui-Jung Hwang. Supervision: Ui-Jung Hwang and Ki-Hwan Kim. Validation: Ui-Jung Hwang and Ki-Hwan Kim. Visualization: Ui-Jung Hwang. Writing – original draft: Ui-Jung Hwang, Byong Jun Min, and Meyoung Kim. Writing – review & editing: Ui-Jung Hwang and Ki-Hwan Kim.

References

1. Grills IS, Hugo G, Kestin LL, Galerani AP, Chao KK, Wloch J, et al. Image-guided radiotherapy via daily online cone-beam CT substantially reduces margin requirements for stereotactic lung radiotherapy. Int J Radiat Oncol Biol Phys. 2008;70:1045-1056.
2. Wortel RC, Incrocci L, Pos FJ, Lebesque JV, Witte MG, van der Heide UA, et al. Acute toxicity after image-guided intensity modulated radiation therapy compared to 3D conformal radiation therapy in prostate cancer patients. Int J Radiat Oncol Biol Phys. 2015;91:737-744.
3. Diao K, Lobos EA, Yirmibesoglu E, Basak R, Hendrix LH, Barbosa B, et al. Patient-reported quality of life during definitive and postprostatectomy image-guided radiation therapy for prostate cancer. Pract Radiat Oncol. 2017;7:e117-e124.
4. Huang K, Palma DA, Scott D, McGregor D, Gaede S, Yartsev S, et al. Inter- and intrafraction uncertainty in prostate bed image-guided radiotherapy. Int J Radiat Oncol Biol Phys. 2012;84:402-407.
5. Jiang SB. Technical aspects of image-guided respiration-gated radiation therapy. Med Dosim. 2006;31:141-151.
6. Kupelian PA, Langen KM, Willoughby TR, Zeidan OA, Meeks SL. Image-guided radiotherapy for localized prostate cancer: treating a moving target. Semin Radiat Oncol. 2008;18:58-66.
7. Foskey M, Davis B, Goyal L, Chang S, Chaney E, Strehl N, et al. Large deformation three-dimensional image registration in image-guided radiation therapy. Phys Med Biol. 2005;50:5869-5892.
8. Button MR, Staffurth JN. Clinical application of image-guided radiotherapy in bladder and prostate cancer. Clin Oncol (R Coll Radiol). 2010;22:698-706.
9. Biancia CD, Yorke E, Kollmeier MA. Image guided radiation therapy for bladder cancer: assessment of bladder mo-

tion using implanted fiducial markers. Pract Radiat Oncol. 2014;4:108-115.
10. Xing L, Thorndyke B, Schreibmann E, Yang Y, Li TF, Kim GY, et al. Overview of image-guided radiation therapy. Med Dosim. 2006;31:91-112.
11. Jaffray D, Kupelian P, Djemil T, Macklis RM. Review of image-guided radiation therapy. Expert Rev Anticancer Ther. 2007;7:89-103.
12. International Atomic Energy Agency (IAEA). Introduction of image guided radiotherapy into clinical practice. Vienna: IAEA. 2019; 16.
13. Verellen D, De Ridder M, Storme G. A (short) history of image-guided radiotherapy. Radiother Oncol. 2008;86:4-13.
14. Haus AG, Pinsky SM, Marks JE. A technique for imaging patient treatment area during a therapeutic radiation exposure. Radiology. 1970;97:653-656.
15. Marks JE, Haus AG. The effect of immobilisation on localisation error in the radiotherapy of head and neck cancer. Clin Radiol. 1976;27:175-177.
16. Papiez L, Timmerman R. Hypofractionation in radiation therapy and its impact. Med Phys. 2008;35:112-118.
17. Mohamoud G, Ryan M, Moseley D. IGRT refresher series: a departmental initiative. J Med Imag Radiat Sci. 2015;46(Suppl 1):S20-S21.
18. Verellen D, De Ridder M, Linthout N, Tournel K, Soete G, Storme G. Innovations in image-guided radiotherapy. Nat Rev Cancer. 2007;7:949-960. Erratum in: Nat Rev Cancer. 2008;8:71.
19. Goyal S, Kataria T. Image guidance in radiation therapy: techniques and applications. Radiol Res Pract. 2014;2014: 705604.
20. Keall PJ, Nguyen DT, O'Brien R, Zhang P, Happersett L, Bertholet J, et al. Review of real-time 3-dimensional image guided radiation therapy on standard-equipped cancer radiation therapy systems: are we at the tipping point for the era of real-time radiation therapy? Int J Radiat Oncol Biol Phys. 2018;102:922-931.
21. Weissbluth M, Karzmark CJ, Steele RE, Selby AH. The stanford medical linear accelerator. Radiology. 1959;72:242-253.
22. Jaffray DA, Drake DG, Moreau M, Martinez AA, Wong JW. A radiographic and tomographic imaging system integrated into a medical linear accelerator for localization of bone and soft-tissue targets. Int J Radiat Oncol Biol Phys. 1999;45:773-789.
23. Hong LX, Chen CC, Garg M, Yaparpalvi R, Mah D. Clinical experiences with onboard imager KV images for linear accelerator-based stereotactic radiosurgery and radiotherapy setup. Int J Radiat Oncol Biol Phys. 2009;73:556-561.
24. Wiehle R, Koth HJ, Nanko N, Grosu AL, Hodapp N. On the accuracy of isocenter verification with kV imaging in stereotactic radiosurgery. Strahlenther Onkol. 2009;185:325-330.
25. Lee SW, Jin JY, Guan H, Martin F, Kim JH, Yin FF. Clinical assessment and characterization of a dual tube kilovoltage X-ray localization system in the radiotherapy treatment room. J Appl Clin Med Phys. 2008;9:1-15.
26. Ma J, Chang Z, Wang Z, Jackie Wu Q, Kirkpatrick JP, Yin FF. ExacTrac X-ray 6 degree-of-freedom image-guidance for intracranial non-invasive stereotactic radiotherapy: comparison with kilo-voltage cone-beam CT. Radiother Oncol. 2009;93:602-608.
27. Srinivasan K, Mohammadi M, Shepherd J. Applications of linac-mounted kilovoltage Cone-beam Computed Tomography in modern radiation therapy: a review. Pol J Radiol. 2014;79:181-193.
28. Oelfke U, Tücking T, Nill S, Seeber A, Hesse B, Huber P, et al. Linac-integrated kV-cone beam CT: technical features and first applications. Med Dosim. 2006;31:62-70.
29. Morin O, Gillis A, Chen J, Aubin M, Bucci MK, Roach M 3rd, et al. Megavoltage cone-beam CT: system description and clinical applications. Med Dosim. 2006;31:51-61.
30. Pouliot J, Bani-Hashemi A, Chen J, Svatos M, Ghelmansarai F, Mitschke M, et al. Low-dose megavoltage cone-beam CT for radiation therapy. Int J Radiat Oncol Biol Phys. 2005;61:552-560.
31. Groh BA, Siewerdsen JH, Drake DG, Wong JW, Jaffray DA. A performance comparison of flat-panel imager-based MV and kV cone-beam CT. Med Phys. 2002;29:967-975.
32. Ma CM, Paskalev K. In-room CT techniques for image-guided radiation therapy. Med Dosim. 2006;31:30-39.
33. Wong JR, Grimm L, Uematsu M, Oren R, Cheng CW, Merrick S, et al. Image-guided radiotherapy for prostate cancer by CT-linear accelerator combination: prostate movements and dosimetric considerations. Int J Radiat Oncol Biol Phys. 2005;61:561-569.
34. Wu M, Keil A, Constantin D, Star-Lack J, Zhu L, Fahrig

R. Metal artifact correction for x-ray computed tomography using kV and selective MV imaging. Med Phys. 2014;41:121910.
35. Khan FM. The physics of radiation therapy. 4th ed. Philadelpia: Lippincott, Willams & Wilkins; 2009:414-424.
36. Khan FM. Treatment planning in radiation oncology. 2 nd ed. Philadelpia: Lippincott, Willams & Wilkins; 2007:178-179.
37. Song KH, Snyder KC, Kim J, Li H, Ning W, Rusnac R, et al. Characterization and evaluation of 2.5 MV electronic portal imaging for accurate localization of intra- and extracranial stereotactic radiosurgery. J Appl Clin Med Phys. 2016;17:268-284.
38. Forrest LJ, Mackie TR, Ruchala K, Turek M, Kapatoes J, Jaradat H, et al. The utility of megavoltage computed tomography images from a helical tomotherapy system for setup verification purposes. Int J Radiat Oncol Biol Phys. 2004;60:1639-1644.
39. Netherton T, Li Y, Gao S, Klopp A, Balter P, Court LE, et al. Experience in commissioning the halcyon linac. Med Phys. 2019;46:4304-4313.
40. Malajovich I, Teo BK, Petroccia H, Metz JM, Dong L, Li T. Characterization of the megavoltage cone-beam computed tomography (MV-CBCT) system on HalcyonTM for IGRT: image quality benchmark, clinical performance, and organ doses. Front Oncol. 2019;9:496.
41. Tang G, Moussot C, Morf D, Seppi E, Amols H. Low-dose 2.5 MV cone-beam computed tomography with thick CsI flat-panel imager. J Appl Clin Med Phys. 2016;17:235-245.
42. Yue Y, Aristophanous M, Rottmann J, Berbeco RI. 3-D fiducial motion tracking using limited MV projections in arc therapy. Med Phys. 2011;38:3222-3231.
43. Azcona JD, Li R, Mok E, Hancock S, Xing L. Automatic prostate tracking and motion assessment in volumetric modulated arc therapy with an electronic portal imaging device. Int J Radiat Oncol Biol Phys. 2013;86:762-768.
44. Tang X, Lin T, Jiang S. A feasibility study of treatment verification using EPID cine images for hypofractionated lung radiotherapy. Phys Med Biol. 2009;54:S1-S8.
45. Shirato H, Shimizu S, Kitamura K, Onimaru R. Organ motion in image-guided radiotherapy: lessons from real-time tumor-tracking radiotherapy. Int J Clin Oncol. 2007;12:8-16.
46. Kashani R, Olsen JR. Magnetic resonance imaging for target delineation and daily treatment modification. Semin Radiat Oncol. 2018;28:178-184.
47. Dawson LA, Sharpe MB. Image-guided radiotherapy: rationale, benefits, and limitations. Lancet Oncol. 2006;7:848-858.
48. Stam MK, Crijns SP, Zonnenberg BA, Barendrecht MM, van Vulpen M, Lagendijk JJ, et al. Navigators for motion detection during real-time MRI-guided radiotherapy. Phys Med Biol. 2012;57:6797-6805.
49. Raaijmakers AJ, Raaymakers BW, Lagendijk JJ. Magnetic-field-induced dose effects in MR-guided radiotherapy systems: dependence on the magnetic field strength. Phys Med Biol. 2008;53:909-923.
50. Raaijmakers AJ, Raaymakers BW, Lagendijk JJ. Integrating a MRI scanner with a 6 MV radiotherapy accelerator: dose increase at tissue-air interfaces in a lateral magnetic field due to returning electrons. Phys Med Biol. 2005;50:1363-1376.
51. Raaijmakers AJ, Raaymakers BW, van der Meer S, Lagendijk JJ. Integrating a MRI scanner with a 6 MV radiotherapy accelerator: impact of the surface orientation on the entrance and exit dose due to the transverse magnetic field. Phys Med Biol. 2007;52:929-939.
52. Raaymakers BW, Raaijmakers AJ, Kotte AN, Jette D, Lagendijk JJ. Integrating a MRI scanner with a 6 MV radiotherapy accelerator: dose deposition in a transverse magnetic field. Phys Med Biol. 2004;49:4109-4118.
53. Stanescu T, Schaer N, Breen S, Letourneau D, Shet K, Dickie CI, et al. Magnetic resonance guided radiation therapy: feasibility study of a linear accelerator and magnetic resonance-on-rails system. Int J Radiat Oncol Biol Phys. 2016;96(Suppl 2):S61-S62.
54. Jaffray DA, Carlone MC, Milosevic MF, Breen SL, Stanescu T, Rink A, et al. A facility for magnetic resonance-guided radiation therapy. Semin Radiat Oncol. 2014;24:193-195.
55. Mutic S, Dempsey JF. The ViewRay system: magnetic resonance-guided and controlled radiotherapy. Semin Radiat Oncol. 2014;24:196-199.
56. Choi CH, Park SY, Kim JI, Kim JH, Kim K, Carlson J, et al. Quality of tri-Co-60 MR-IGRT treatment plans in comparison with VMAT treatment plans for spine SABR. Br J Radiol. 2017;90:20160652.
57. Klüter S. Technical design and concept of a 0.35 T MR-

Linac. Clin Transl Radiat Oncol. 2019;18:98-101.
58. Raaymakers BW, Jürgenliemk-Schulz IM, Bol GH, Glitzner M, Kotte ANTJ, van Asselen B, et al. First patients treated with a 1.5 T MRI-Linac: clinical proof of concept of a high-precision, high-field MRI guided radiotherapy treatment. Phys Med Biol. 2017;62:L41-L50.
59. Raaymakers BW, Lagendijk JJ, Overweg J, Kok JG, Raaijmakers AJ, Kerkhof EM, et al. Integrating a 1.5 T MRI scanner with a 6 MV accelerator: proof of concept. Phys Med Biol. 2009;54:N229-N237.
60. Winkel D, Bol GH, Kroon PS, van Asselen B, Hackett SS, Werensteijn-Honingh AM, et al. Adaptive radiotherapy: The Elekta Unity MR-linac concept. Clin Transl Radiat Oncol. 2019;18:54-59.
61. Keall PJ, Barton M, Crozier S. The Australian magnetic resonance imaging-linac program. Semin Radiat Oncol. 2014;24:203-206.
62. Fallone BG. The rotating biplanar linac-magnetic resonance imaging system. Semin Radiat Oncol. 2014;24:200-202.
63. Cusumano D, Boldrini L, Dhont J, Fiorino C, Green O, Güngör G, et al. Artificial Intelligence in magnetic Resonance guided Radiotherapy: medical and physical considerations on state of art and future perspectives. Phys Med. 2021;85:175-191.
64. Langen KM, Pouliot J, Anezinos C, Aubin M, Gottschalk AR, Hsu IC, et al. Evaluation of ultrasound-based prostate localization for image-guided radiotherapy. Int J Radiat Oncol Biol Phys. 2003;57:635-644.
65. Scarbrough TJ, Golden NM, Ting JY, Fuller CD, Wong A, Kupelian PA, et al. Comparison of ultrasound and implanted seed marker prostate localization methods: implications for image-guided radiotherapy. Int J Radiat Oncol Biol Phys. 2006;65:378-387.
66. Camps SM, Fontanarosa D, de With PHN, Verhaegen F, Vanneste BGL. The use of ultrasound imaging in the external beam radiotherapy workflow of prostate cancer patients. Biomed Res Int. 2018;2018:7569590.
67. Richardson AK, Jacobs P. Intrafraction monitoring of prostate motion during radiotherapy using the Clarity® Autoscan Transperineal Ultrasound (TPUS) system. Radiography (Lond). 2017;23:310-313.
68. Lachaine M, Falco T. Intrafractional prostate motion management with the Clarity Autoscan System. Med Phys Int J. 2013;1:72-80.
69. Baker M, Behrens CF. Prostate displacement during transabdominal ultrasound image-guided radiotherapy assessed by real-time four-dimensional transperineal monitoring. Acta Oncol. 2015;54:1508-1514.
70. Brahme A, Nyman P, Skatt B. 4D laser camera for accurate patient positioning, collision avoidance, image fusion and adaptive approaches during diagnostic and therapeutic procedures. Med Phys. 2008;35:1670-1681.
71. Pallotta S, Marrazzo L, Ceroti M, Silli P, Bucciolini M. A phantom evaluation of Sentinel™, a commercial laser/camera surface imaging system for patient setup verification in radiotherapy. Med Phys. 2012;39:706-712.
72. Hoisak JDP, Pawlicki T. The role of optical surface imaging Systems in Radiation Therapy. Semin Radiat Oncol. 2018;28:185-193.
73. Hattel SH, Andersen PA, Wahlstedt IH, Damkjaer S, Saini A, Thomsen JB. Evaluation of setup and intrafraction motion for surface guided whole-breast cancer radiotherapy. J Appl Clin Med Phys. 2019;20:39-44.
74. Kügele M, Edvardsson A, Berg L, Alkner S, Andersson Ljus C, Ceberg S. Dosimetric effects of intrafractional isocenter variation during deep inspiration breath-hold for breast cancer patients using surface-guided radiotherapy. J Appl Clin Med Phys. 2018;19:25-38.
75. Lee SK, Huang S, Zhang L, Ballangrud AM, Aristophanous M, Cervino Arriba LI, et al. Accuracy of surface-guided patient setup for conventional radiotherapy of brain and nasopharynx cancer. J Appl Clin Med Phys. 2021;22:48-57.
76. Li G, Ballangrud A, Kuo LC, Kang H, Kirov A, Lovelock M, et al. Motion monitoring for cranial frameless stereotactic radiosurgery using video-based three-dimensional optical surface imaging. Med Phys. 2011;38:3981-3994.
77. Walter F, Freislederer P, Belka C, Heinz C, Söhn M, Roeder F. Evaluation of daily patient positioning for radiotherapy with a commercial 3D surface-imaging system (Catalyst™). Radiat Oncol. 2016;11:154.
78. Kügele M, Mannerberg A, Nørring Bekke S, Alkner S, Berg L, Mahmood F, et al. Surface guided radiotherapy (SGRT) improves breast cancer patient setup accuracy. J Appl Clin Med Phys. 2019;20:61-68.
79. Stanley DN, McConnell KA, Kirby N, Gutiérrez AN, Papa-

nikolaou N, Rasmussen K. Comparison of initial patient setup accuracy between surface imaging and three point localization: a retrospective analysis. J Appl Clin Med Phys. 2017;18:58-61.

80. Chow VUY, Cheung MLM, Kan MWK, Chan ATC. Shift detection discrepancy between ExacTrac Dynamic system and cone-beam computed tomography. J Appl Clin Med Phys. 2022;23:e13567.
81. Das S, Liu T, Jani AB, Rossi P, Shelton J, Shi Z, et al. Comparison of image-guided radiotherapy technologies for prostate cancer. Am J Clin Oncol. 2014;37:616-623.
82. Willoughby TR, Kupelian PA, Pouliot J, Shinohara K, Aubin M, Roach M 3rd, et al. Target localization and real-time tracking using the Calypso 4D localization system in patients with localized prostate cancer. Int J Radiat Oncol Biol Phys. 2006;65:528-534.
83. Ogunleye T, Rossi PJ, Jani AB, Fox T, Elder E. Performance evaluation of Calypso 4D localization and kilovoltage image guidance systems for interfraction motion management of prostate patients. ScientificWorldJournal. 2009;9:449-458.
84. Rajendran RR, Plastaras JP, Mick R, McMichael Kohler D, Kassaee A, Vapiwala N. Daily isocenter correction with electromagnetic-based localization improves target coverage and rectal sparing during prostate radiotherapy. Int J Radiat Oncol Biol Phys. 2010;76:1092-1099.